Available online at www.sciencedirect.com
SCIENCE DIRECT®
Journal of Sound and Vibration 292 (2006) 694–709
JOURNAL OF SOUND AND VIBRATION
www.elsevier.com/locate/jsvi

Design and performance evaluation of a serial multi-electrode electrorheological damper

Wen-Hwar Kuo[a,b,*], Tsong-Neng Wu[c], Jenhwa Guo[c], Mao-Hsiung Chiang[d], Yi-Nan Chen[c]

[a]*Department of Mechanical Engineering, National Taiwan University, Taipei, Taiwan 106, ROC*
[b]*Department of Automation Engineering, Tung Nan Institute of Technology, Taipei, Taiwan 222, ROC*
[c]*Department of Engineering Science and Ocean Engineering, National Taiwan University, Taipei, Taiwan 106, ROC*
[d]*Institute of Automation and Control, National Taiwan University of Science and Technology, Taiwan 106, ROC*

Received 12 November 2003; received in revised form 16 June 2005; accepted 26 August 2005
Available online 5 January 2006

Abstract

This study presents the design and performance evaluation of a serial multi-electrode electrorheological (SMER) damper. The characteristics of electrorheological (ER) fluid and SMER damper are experimentally obtained. The design method for ER dampers is based on the requirements of the system damper such as controllable damping force, controllable ratio and the ratio of rebound damping force and compression damping force. Then the SMER damper is applied to the single-degree-of-freedom model of a vibration system to evaluate the performance of an SMER damper. The vibration control system uses a velocity control algorithm. The simulation and experimental response of the displacement as well as the acceleration indicate the effectiveness of the design of the SMER damper.

1. Introduction

Electrorheological (ER) fluids are polarized particles mixed with non-conducting liquids. When subject to an electric field, the viscosity and yield shear stress of the liquid increases with the electric field strength to such an extent that the liquid may become plastic within response time of approximately a few milliseconds. The plastic quickly turns into liquid again once the electric field is removed. This phenomenon of ER fluids is so-called ''ER effect'' [1,2]. ER fluids offer the potential for achieving easily controlled, fast acting, continuously variable dampers, using the continuously variable damping forces that can be obtained from suitable ER device [3]. Unlike an electromechanical valve, an ER valve can achieve flow control without moving parts in fluid control systems. Many researchers have studied the characteristics and applications of ER fluids. Because of their fast response to the electric field and wide control bandwidth, ER fluids can be used for controllable dampers and control systems [4].

*Corresponding author. Department of Mechanical Engineering, National Taiwan University, Taipei, Taiwan 106, ROC.
E-mail address: whkuo@mail.tnit.edu.tw (W.-H. Kuo).

0022-460X/$ - see front matter © 2005 Elsevier Ltd. All rights reserved.
doi:10.1016/j.jsv.2005.08.035

In order to improve the controllable damping force of ER dampers using low effective ER fluids, some researchers have used high viscosity ER grease dampers, long electrode stroke dampers or multi-electrode dampers to conduct experiments. For example, Marksmeier et al. [5,6] used high viscosity ER grease in their studies, developing a concentric electrode ER damper with a tested stroke of 0.02 m and a controllable force range from 0.6 to 0.7 kN at 0.3 m/s. Although the damping force can be promoted, the damping force of zero-field will be too high to make the controllable range of applied electric field relatively low. Sims et al. [7] developed a long-stroke ER damper with a single bypass valve and tested it with commercial ER material. This damper had a tested stroke of 0.016 m with a controllable force range from 1.2 to 3.8 kN at 0.2 m/s. Gavin [8] developed a multi-duct ER damper with a long electrode length of 0.235 m and electrode outside diameter 0.08 m. He tested a stroke of 0.08 m with a controllable force range from 2 to 6 kN at 0.25 m/s using a serial duct ER damper. However, the long stroke ER damper is restricted with its space in actual use.

Mui et al. [9] developed a parallel multi-electrode ER damper. This damper has a tested stroke of 0.01 m with a damping force 0.02 kN at 0.063 m/s when tested with a zeolite-based ER material. Makris et al. [10] developed an ER damper with a bypass ER valve. This damper has a tested stroke of 0.02 m with a controllable force range from 0.2 to 0.3 kN at 0.013 m/s with a zeolite-based ER fluid tested. The damping force of the damper and its controllable force range are very small, so the multi-electrode parallel to damping force and its controllable force range are also not very large. This can be demonstrated by the parallel multi-electrode ER damper studied by Kuo et al. [11], who used ER fluid mixed with silicone oil and corn starch. Gavin [8,12] studied numerical examples to focus on a large-scale damper, and showed that a simulated damper can regulate very large forces. He designed, tested and modeled three multi-duct ER dampers, which have controllable force levels from 2 to 6 kN at 0.4 m/s when tested with commercial ER fluids. Gavin also studied a large-scale and long-stroke damper applied to civil engineering, which has two piston rods in the cylinder. The SMER damper in this study has a tested stroke of 0.1 m and a hydraulic serial ER dampers, the controllable damping force is from 0.7 to 1.4 kN with 3-layer ER damper. If we use a 5-layer ER damper with electrode gap $h = 0.6$ mm, the damping force is from 1.32 to 3.6 kN at the rebound stroke.

The ER damper is a device with controllable damping force or damping coefficient, which can be applied to control vibration systems or semi-active suspension systems. For instance, in their studies, Wong et al. [13] and Wu et al. [14] used a parallel multi-electrode ER damper as well as various composite control strategies to improve both ride comfort and road holding. Brennan et al. [15] described the design and testing of a rotary vibration damper using ER fluid in the shear mode for a semi-active control system. Weyenberg et al. [4] applied ER dampers to the semi-active suspension systems of vehicles controlled by a modified sky-hook algorithm, and directly installed accelerometers and position sensors in vehicles to measure the feedback signals of the vehicles. The results showed that the level of vehicle body acceleration and the tire load variation were improved. Nakano [16] constructed a quarter car suspension system model and proposed several semi-active control algorithms for ER damper, which showed that the proportional feedback control using the information of absolute unsprung mass velocity is the most effective control strategy. Gordaninejad et al. [17] evaluated the performance of multi-electrode shear mode ER dampers under forced vibration through experiment, demonstrating the effects of the number of electrodes and electrode surface area of ER dampers. Choi et al. [18] proposed a cylindrical ER damper for a passenger car which showed that a continuously variable ER damper can be satisfactorily used for the feedback control of desired damping forces. Its controllability of damping force was improved by implementing a skyhook controller. Suh et al. [19] used a sky-hook control algorithm to improve the ride quality through computer simulation, and then the ER damper was installed in a passenger car for testing. The results of the experiment showed that the rms acceleration of control mode was generally better than that of passive mode. Onoda et al. [20] fabricated an ER damper and investigated the effectiveness of semi-active vibration suppression. Choi et al. [21] adopted the hardware-in-the-loop simulation method and used a sliding mode controller. The simulation results showed that the full-car ER suspension system was very effective for vibration isolation. Choi et al. [22] evaluated the performance characteristics of a semi-active ER suspension system associated with a skyhook controller and four ER shock absorbers to a full car. Their results showed that the semi-active system could be effectively employed in a passenger vehicle, improving both riding comfort and steering stability. Oh et al. [23] designed and fabricated an MR damper for semi-active vibration suppression, and their results showed that the performance of the MR damper was better than that of the ER damper.

From these previous studies, it is clear that most ER dampers are long-stroke (long-electrode) dampers, parallel multi-electrode flow mode ER dampers or multi-electrode shear mode ER dampers. This type of ER damper is a serial multi-electrode ER (SMER) damper, which is suitable for use as a short stroke damper with high damping coefficient. The SMER damper consists of a set of concentric cylindrical electrodes, which are electrically parallel and with flow paths arranged in series hydraulically. Hence the stroke of this ER damper is short, so it can improve the ER effect. This is different from the parallel multi-electrode ER damper. According to the researches of Kuo [11] and Chen [24], the variable damping force or coefficient of the parallel multi-electrode ER damper is less than that of single-electrode ER damper. Choi et al. [25] designed an orifice-type ER damper that was also suitable for use as a short stroke damper, but the piston design was very complicated.

Ordinary vehicle dampers need different relative amounts of compression and rebound damping force for riding quality. On passenger cars, the relative amount of compression and rebound damping vary between 20/80 and 50/50, but tends to be around 30/70. On motorcycles, the ratio seems to be even more asymmetric, perhaps from 20/80 to 5/95 [26]. For these purposes, we have analyzed the mechanism to adjust the relative amounts of compression and rebound damping in SMER dampers. The purpose of this paper is to investigate the characteristics of SMER dampers and to experimentally demonstrate the effectiveness of the controlled vibration suppression using an SMER damper. In addition, the design method for ER dampers based on technical requirements of the damper such as controllable damping force, controllable ratio and the ratio of rebound damping force and compression damping force is also described. Section 2 focuses on the design and performance evaluation of an SMER damper, and its behavior is mathematically modeled. Section 3 presents the characteristics of our ER fluid and the SMER damper. ER fluid characteristics are examined using an electrorheometer, and they are represented by incorporating Bingham plastic models. In Section 4, the SMER damper is applied to a single-degree-of-freedom (SDOF) model of vibration system to evaluate the performance of control vibration system using a velocity control algorithm. The controller is designed such that the control voltage is proportional to the absolute velocity of the sprung mass. The SMER damper is shown to be effective to control the vibration motion.

2. SMER damper

Fig. 1 shows an SMER damper with an innermost ER valve. This device consists of a set of concentric cylindrical electrodes and a concentric piston within the inner electrodes. All the electrodes are electrically parallel and the flow paths are arranged in series hydraulically. With every electrode gap denoted by h_e, its electrode length by L_e, and its average diameter of every electrode gap is d_{ei}, $i = 1, 2 \ldots n$, and the viscosity of ER fluid is μ.

Mathematically, the total damping force F of the SMER damper is given as

$$F = F_a + F_{erv} + F_g + F_{fs}. \tag{1}$$

(a) The inertial force F_a represents piston acceleration $\ddot{y}$ i.e. $F_a = m\ddot{y}$. It is very small compared to the damping force, thus it can be ignored, i.e. $F_a = 0$.

(b) The damping force F_{erv} due to pressure drop of SMER valve is proportional to the cross-sectional area of piston head A and the pressure drop ΔP_{ns} developed by SMER valve, i.e.

$$F_{erv} = A(\Delta P_{ns}). \tag{2}$$

The pressure drop ΔP_{ns} is the sum of the pressure drop ΔP_v developed by the hydraulic series annular gap without applying electric field and the pressure drop ΔP_e influenced by ER effect with applying electric field. The total pressure drop ΔP_{ns} of n-layer SMER valve is illustrated by the following equation [27]:

$$\Delta P_{ns} = \Delta P_v + \Delta P_e = C_v \sum_{i=1}^{n} \left(\frac{1}{d_{ei}}\right) Q_e + nC_e\tau_y, \tag{3}$$

where $C_v = 12\mu L_e/\pi h_e^3$, $C_e = 2L_e/h_e$ and Q_e is the flow rate through all electrode gaps.

From Wolff-Jesse and Fees [28] and our own numerous experiments with ER dampers, the actual flow behavior of the ER fluid is influenced by not only the electrical field E (V/mm) and the coefficient of ER fluid

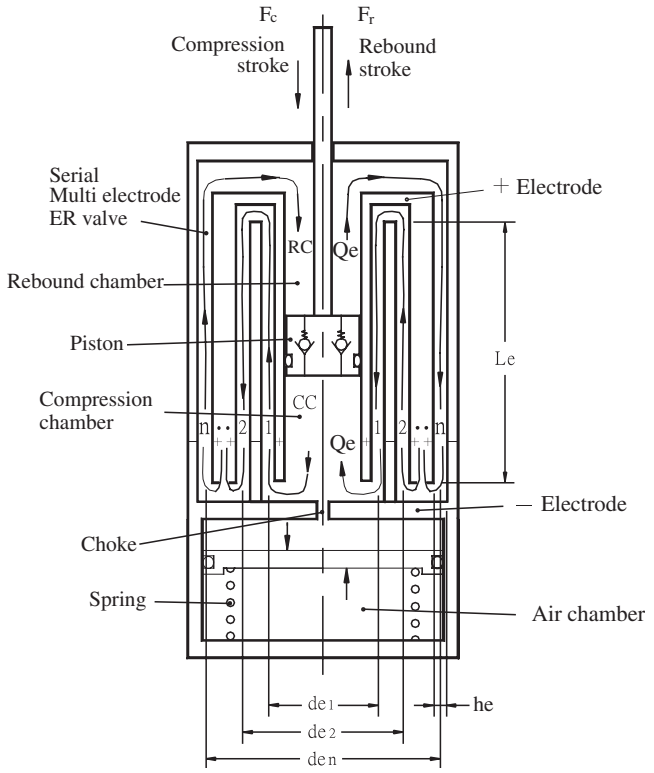

Fig. 1. The n-layer SMER damper.

material but also the flow velocity of the electrode median gap v (m/s). Thus the yield shear stress τ_y of ER valve is here approximated by the simple function:

$$\tau_y = \tau(E, v) = \alpha E^{\beta} + \alpha E^{\beta}(v^{\psi}), \tag{4}$$

where α and β are the coefficients of the ER material, and Ψ is an exponent. In addition,

$$\Delta P_{ns} = \left[C_v \sum_{i=1}^{n} \left(\frac{1}{d_{ei}} \right) A \right] \dot{y} + nC_e\alpha(E^{\beta} + G_s \dot{y}^{\Psi} E^{\beta}), \tag{5}$$

where $G_s = (nA/\pi h_e \sum_{i=1}^{n} d_{ei})^{\Psi}$, and A is the cross-sectional area of piston head. If the SMER damper is at the compression stroke, $A = A_c$; and at the rebound stroke, $A = A_r$. $A_c = \pi d_p^2/4$, $A_r = A_c - A_{\text{rod}}$, where A_{rod} is the cross-sectional area of the piston rod, $A_r = \pi d_{\text{rod}}^2/4$. d_{rod} is the diameter of piston rod.

Using the model of the pressure drop of (i) the serial multi-electrode ER (SMER) valve (ΔP_{ns}), (ii) the single-electrode ER valve (ΔP_1), and (iii) the parallel multi-electrode ER (PMER) valve (ΔP_{np}) analyzed by Kuo et al. [27], the relationship of the pressure drop and the electric field of these three valves can be obtained. Let the electrode length $L_e = 100$ mm, the electrode gap $h_e = 1$ mm, the average diameter of every electrode gap $d_{e1} = 18.5$ mm, $d_{e2} = 23.5$ mm, $d_{e3} = 28.5$ mm, $d_{e4} = 33.5$ mm, $d_{e5} = 38.5$ mm and the electrode number $n = 1$ to 5 of SMER valves and PMER valves. The controllable pressure drop is defined as $\Delta P_E - \Delta P_0$, and the controllable ratio (CR) is defined as the ratio of $(\Delta P_E - \Delta P_0)/\Delta P_0$, where ΔP_0 is the pressure drop without applying an electric field, and ΔP_E is the pressure drop when applying the maximum electric field. The analysis results show that the controllable pressure drop of SMER valve is the maximum, i.e. $\Delta P_{ns} > \Delta P_1 > \Delta P_{np}$, and the controllable pressure drop of PMER valve is the minimum, as shown in Fig. 2. The damping force is

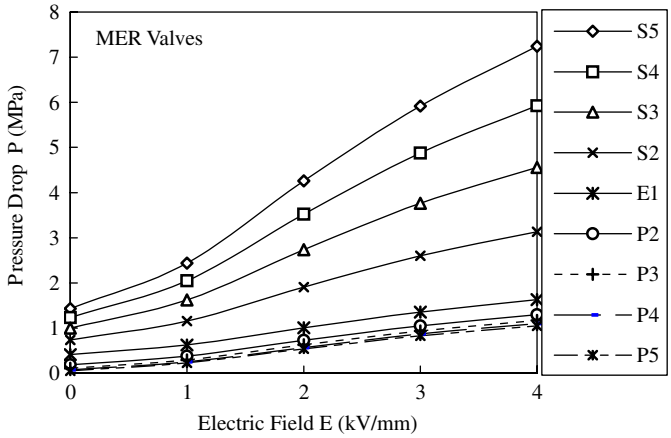

Fig. 2. The controllable pressure drop of three kinds of ER valves; S2–S5: electrode number 2–5 of SMER valve; P2–P5: electrode number 2–5 of PMER valve; E1: single electrode ER valve.

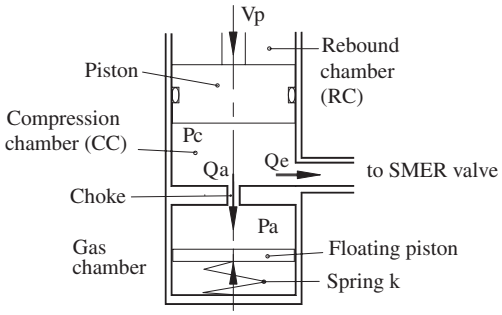

Fig. 3. Gas chamber of SMER damper.

proportional to the pressure drop of the ER valve, so the damping force of SMER damper is larger than that of single-electrode ER damper, and larger than that of PMER damper.

(c) The damping force F_g due to the gas compliance is the pressure P_a of the gas chamber and the pressure P_c of the compression chamber.

$$F_g = A_{\text{rod}} P_c, \tag{6}$$

where A_{rod} is the cross-sectional area of piston rod, P_c can be obtained from analysis of Fig. 3 as follows.

When the piston rod goes into the rebound chamber at a compression stroke, the volume increment by the piston rod may flow through the choke to the gas chamber. As fluid in the compression chamber flows through the small diameter and the long length choke to the gas chamber [29], the pressure drop equation can be obtained as

$$\Delta P_{ca} = P_c - P_a = \frac{128 \mu l_a}{\pi d_a^4} Q_a, \tag{7}$$

where d_a is the diameter of choke, l_a the length of choke, and P_{air} the pressure of the gas chamber. The flow rate of piston compression stroke $Q_c = A_c \dot{y}$ is sum of the flow rate Q_e through all electrode gaps and the flow rate Q_a through the gas chamber.

$$Q_c = Q_e + Q_a = A_c \dot{y}, \tag{8}$$

$$Q_a = A_{\text{rod}} \dot{y}, \tag{9}$$

$$Q_e = A_r \dot{y}. \tag{10}$$

The gas chamber has a floating piston, with piston diameter of d_{air} and the floating piston area is A_{air}. In addition, y_{air} is the compression length of spring compressed by the floating piston which is supported by a spring. The spring coefficient is k, and pre-compression length of the spring is x_0. From the force balance equation of the floating piston,

$$F_{ap} = (y_{\text{air}} + x_0)k = P_a A_{\text{air}}. \tag{11}$$

From Eqs. (7), (9), (10) and the equation of state for gas in the gas chamber $P_i V_i^{\gamma} = P_f V_f^{\gamma}$, the pressure P_c of the compression chamber can be derived. Considering the initial pressure P_i and initial volume V_i in the gas chamber, the pressure P_c of the compression chamber can be obtained.

$$P_c = \frac{kx_0}{A_{air}} + k\left(\frac{A_{\text{rod}}}{A_{\text{air}}^2}\right)y + \frac{P_i V_i^{\gamma}}{[V_i - (y - y_0)A_{\text{rod}}]^{\gamma}} + \left(\frac{128\mu l_a A_{\text{rod}}}{\pi d_a^4}\right)\dot{y}. \tag{12}$$

In the above equation, P_f and V_f are the pressure and volume after compression of the floating piston, and γ is the specific heat ratio.

The Coulomb friction and viscous resistance force, F_{fs}, are developed by the piston and the piston rod. The force, F_{fs}, is influenced by the Coulomb friction force, the viscosity of ER fluid and the piston velocity $\dot{y}$. It can be obtained by experiment, and here approximated by the simple function:

$$F_{fs} = f_{fs}|\dot{y}|^{\phi}, \tag{13}$$

where f_{fs} is the frictional force constant, and ϕ is the exponent.

In order to change the relative amounts of compression and rebound damping force, we have redesigned the piston of SMER damper to make the damping force of compression stroke less than that of rebound stroke. The check valve can enable the free flow from the compression chamber to the rebound chamber, and the diameter of the check valve can adjust the relative amounts of compression and rebound damping force in SMER dampers. Fig. 4 shows SMER damper with the check valve of piston. When the SMER damper is at the compression stroke, the fluid flows from the compression chamber to the rebound chamber through the SMER valve and the check valve of piston. The major flow rate flows through the check valve, so the damping force developed by SMER valve is very small. The pressure drop ΔP_{ns} of the compression stroke is changed to $\Delta P_{ns(ckv)}$.

$$\Delta P_{ns(ckv)} = C_v \sum_{i=1}^{n}\left(\frac{1}{d_{ei}}\right)Q_{ec} + nC_e\tau_y. \tag{14}$$

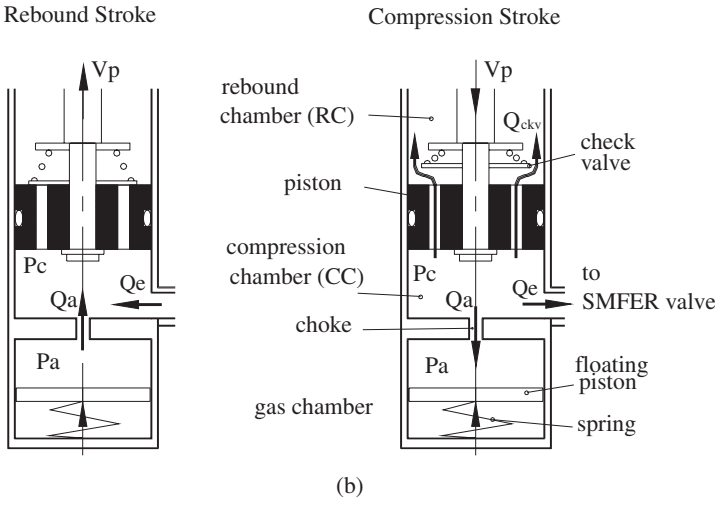

Fig. 4. The SMER damper with the check valve of the piston. (a) Rebound stroke, and (b) compression stroke.

The flow rate through SMER valve is,

$$Q_{ec} = A_c\dot{y} - Q_a - Q_{ckv} = A_r\dot{y} - Q_{ckv}. \tag{15}$$

The choke flow rate of check valve is,

$$Q_{ckv} = \left(\frac{\pi d_{ckv}^4}{128\mu l_{ckv}}\right)\Delta P_{ns(ckv)}. \tag{16}$$

From Eqs. (14) to (16), the pressure drop $\Delta P_{ns(ckv)}$ of the compression stroke can be obtained as

$$\Delta P_{ns(ckv)} = \left[\frac{1}{1 + C_v\sum_{i=1}^{n}(1/d_{ei})(\pi d_{ckv}^4/32\mu l_{ckv})}\right]\left[C_v\sum_{i=1}^{n}\left(\frac{1}{d_{ei}}\right)A_r\dot{y} + nC_e\tau_y\right]. \tag{17}$$

The pressure drop ΔP_{ns} of the rebound stroke is

$$\Delta P_{ns} = C_v\sum_{i=1}^{n}\left(\frac{1}{d_{ei}}\right)A_r\dot{y} + nC_e\tau_y. \tag{18}$$

If we neglect the modulated force F_g and the Coulomb friction and viscous resistance force F_{fs} of the piston and the piston rod, then the damping force ratio R_d of compression and rebound stroke without applied electric field is

$$R_d = \frac{F_{c0}}{F_{r0}} = \frac{A_c(\Delta P_{ns(ckv)})}{A_r(\Delta P_{ns})} = \left(\frac{A_c}{A_r}\right)\left(\frac{1}{1 + C_v\sum_{i=1}^{n}(1/d_{ei})(4\pi/128\mu l_{ckv})d_{ckv}^4}\right). \tag{19}$$

We simulate the damping characteristics of the SMER damper using the check valve of the piston for electrode numbers 3 and 3 Hz exciting frequency. The check valve has 4 chokes, and each diameter has $d_{ckv} = 0.0012$ m. The cracking pressure is 0.05 Mpa. Fig. 5 shows the relationship of the damping force ratio R_d and choke diameter d_{ckv} of the piston from Eq. (19).

Using the mathematical model, the simulated damping force is shown in Fig. 6 for the 5-layer SMER damper with $L = 200$ mm and $h_e = 1$ mm. Fig. 7 shows the characteristics of the 3-layer SMER damper with $L = 100$ mm and $h_e = 0.6$ mm from simulation.

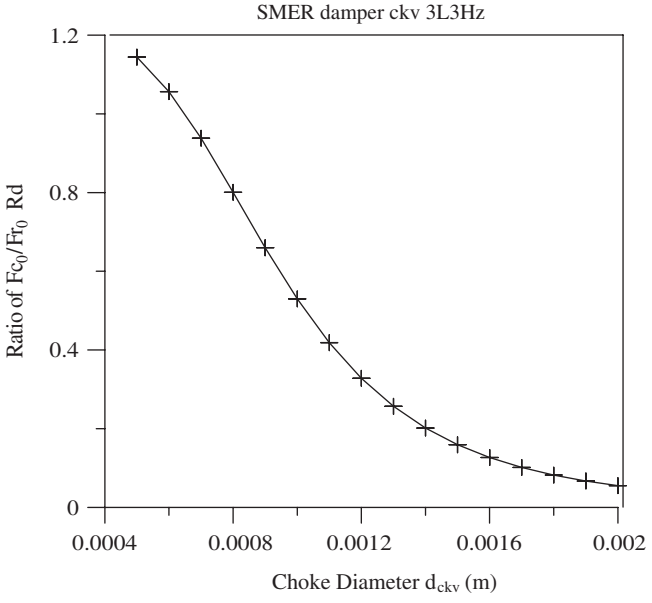

Fig. 5. The relationship of the damping force ratio of F_{c0}/F_{r0} and the choke diameter of SMER damper with the check valve.

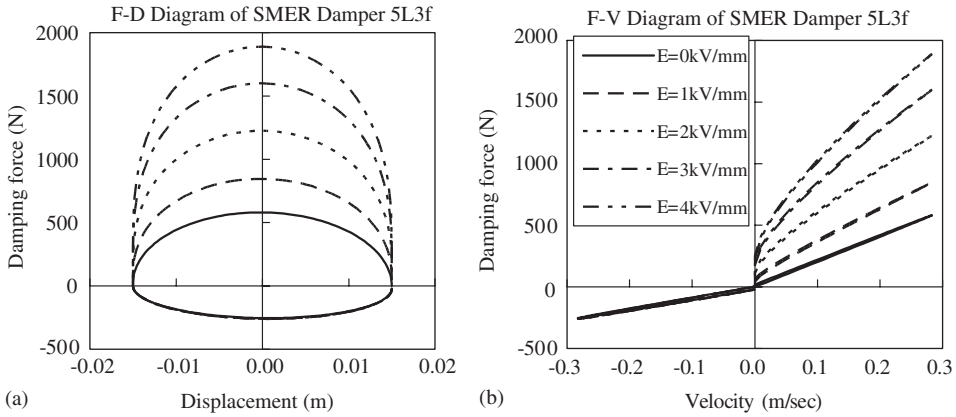

Fig. 6. Simulated characteristics of the 5-layer SMER damper. (a) *F–D* diagram, and (b) *F–V* diagram.

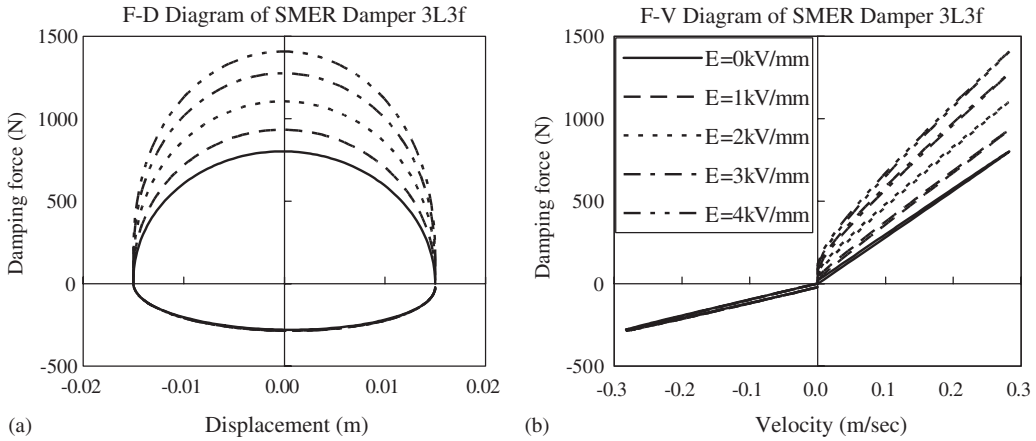

Fig. 7. Simulated characteristics of the 3-layer SMER damper. (a) *F–D* diagram, and (b) *F–V* diagram.

The damping coefficient C is defined as the ratio of the maximum damping force and the maximum velocity. C_r and C_c are the damping coefficients of the rebound and compression stroke, respectively. The relationship between damping coefficient and electric field of the SMER damper with the check valve of the piston at 3 Hz exciting frequency is shown in Fig. 8.

The damping force of ER damper is mainly the sum of the viscous resistance force of ER fluid F_0 and the yield force ($F_E - F_0$) of ER effect with applying electric field. The controllable ratio (CR) is defined as the ratio of the yield force of ER effect with applying electric field and the viscous resistance of fluid, i.e. $(F_E - F_0)/F_0$, F_0 is the damping force without applying electric field, and F_E is the damping force with applying maximum electric field. Because the geometric size of electrode can influence the viscous resistance of fluid and the yield force of ER effect with applying electric field, it may change the controllable ratio. Our design method can provide the suitable geometric sizes of electrode for maximum controllable ratio and damping force, as shown in Fig. 9.

3. Characteristics of ER fluid and SMER damper

The ER fluid in this study is mixed with silicone oil and specially treated 33wt% corn starch. The viscosity of silicone oil is about 100 cPs. In order to evaluate the characteristics and performance of this ER fluid, an

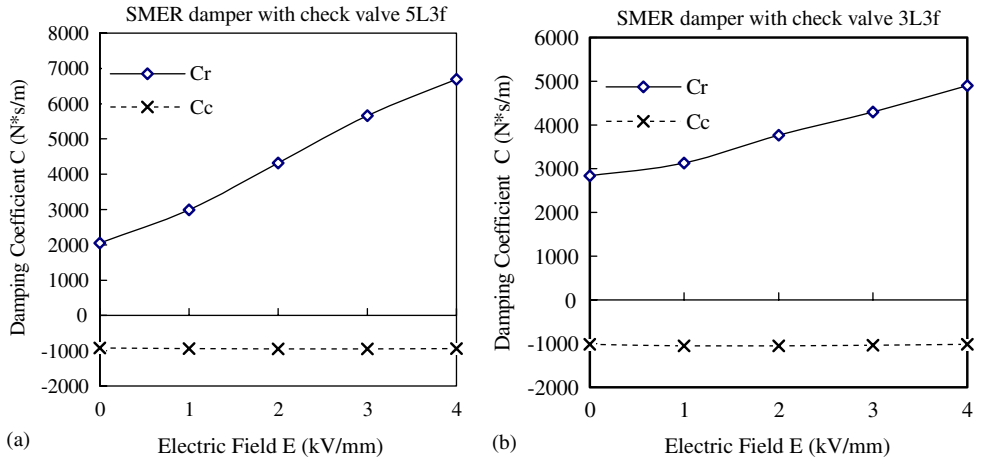

Fig. 8. The damping coefficient of SMER damper with the check valve at 3 Hz exciting frequency: (a) electrode number $n = 5$, $L = 200$ mm, $h = 1$ mm; and (b) electrode number $n = 3$, $L = 100$ mm, $h = 0.6$ mm.

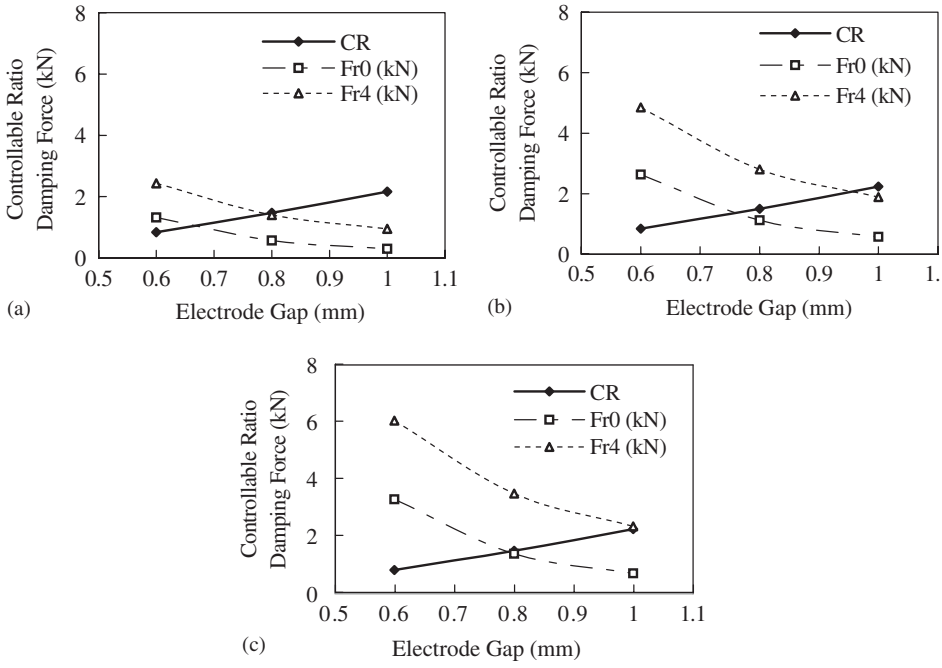

Fig. 9. The relationship of controllable ratio (CR), damping force and geometric electrode size of SMER damper with the check valve, Le = electrode length, L = electrode number, f = frequency. (a) Electrode length Le = 0.1 m, (b) electrode length Le = 0.2 m, and (c) electrode length Le = 0.25 m.

electrorheometer, model NTU ERM-02, was designed, to test the Bingham characteristics and time response of the ER fluid. This device is a concentric cylinder viscometer of Searle type. The influence of the electric field on the yield shear stress can be approximated mathematically and described through the following function by the experiments:

$$\tau_{y0} = 581.5E^{1.175}, \tag{20}$$

where τ_{y0} is the yield shear stress (Pa), and E the electric field (kV/mm). The viscosity of ER fluid is about 200 cPs.

As an electric field is applied to ER fluids, particles chained between electrodes are generated to resist the flow. The formulating and releasing processes of the particle chains under an electric field take some time for the particles to move, a delay of response time occurs, and this time delay has to be considered to design a control vibration system for real-time control. The response time of ER fluid is required to test for controlling vibration systems. The time constant is evaluated to be about 40–50 ms using step responses generated by the electrorheometer.

In order to meet our hydraulic servo-dynamic system capability, we designed and manufactured a 3-layer SMER damper with $L = 100$ mm and $h_e = 0.6$ mm only for experimental study. In this design, the SMER damper is installed on a hydraulic servo-dynamic tester. The top of the ER damper is connected to a 10 kN capacity load cell which, in turn, is mounted to a base excited by a servo-valve cylinder. A 30 cm Novotechnik linear motion transducer is mounted to the exciting cylinder rod and table frame to monitor the displacement and velocity. All data is collected using a National Instruments' data acquisition board and a personal computer. System control and data monitoring are accomplished with LabVIEW 6.9.2. [30]. The high voltage power supply and amplifier is a TREK' HV Power Supply.

The SMER damper experiment was performed at frequencies of 1–5 Hz. At each frequency, tests were performed sequentially for electric fields of 1, 2, 3 and 4 kV/mm, and a peak-to-peak displacement of 0.03 m. The damping force characteristics of the test results and simulations are shown in Fig. 10 at frequency 3 Hz. It can be seen that the experimental data match well to the simulation results.

Time response characteristics can be evaluated with respect to the electric field and the excited motion, indicating how fast one can produce required damping forces by applying high frequency control voltage. The motion of the SMER damper is excited by the triangular wave displacement of ± 7.5 mm at 1 Hz frequency, as shown in Fig. 11(a), and it has a constant damping force at a constant velocity 0.03 m/s, as shown in Fig. 11(b). We applied a square wave control electric field 0–4 kV/mm at 5 Hz frequencies, as shown in Fig. 11(c). The time response characteristics of the SMER damper to square wave control electric field are shown in Fig. 11(b). Fig. 11(d) is the partially enlarged diagram of (b). From Fig. 11(d), the response time is evaluated about 65 ms, which depends on both the response characteristics of the ER fluid itself and also the size of the ER damper.

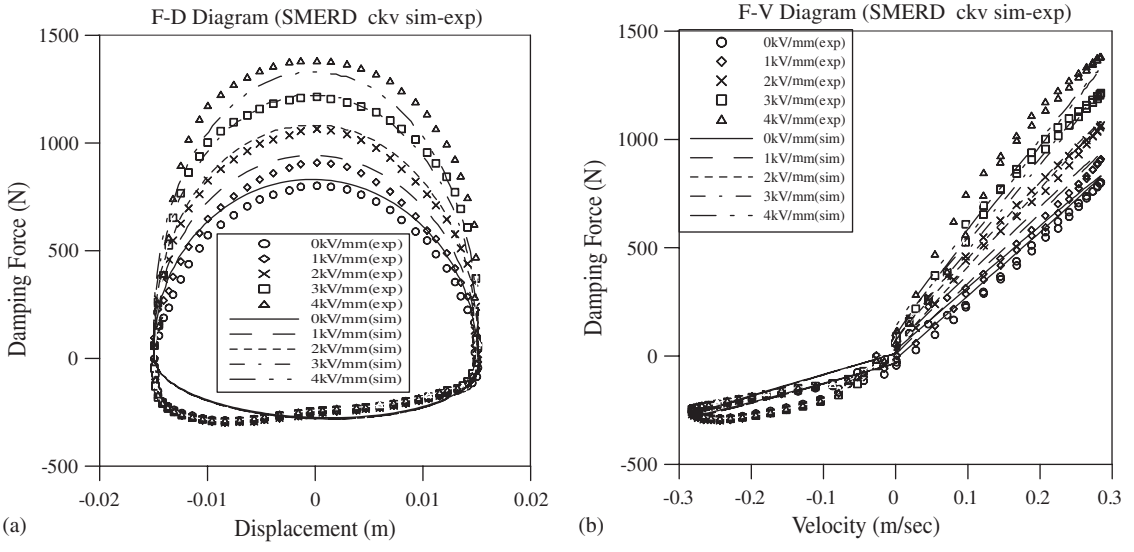

Fig. 10. Simulated and experimentally measured characteristics of the SMER damper. (a) *F–D* diagram and (b) *F–V* diagram.

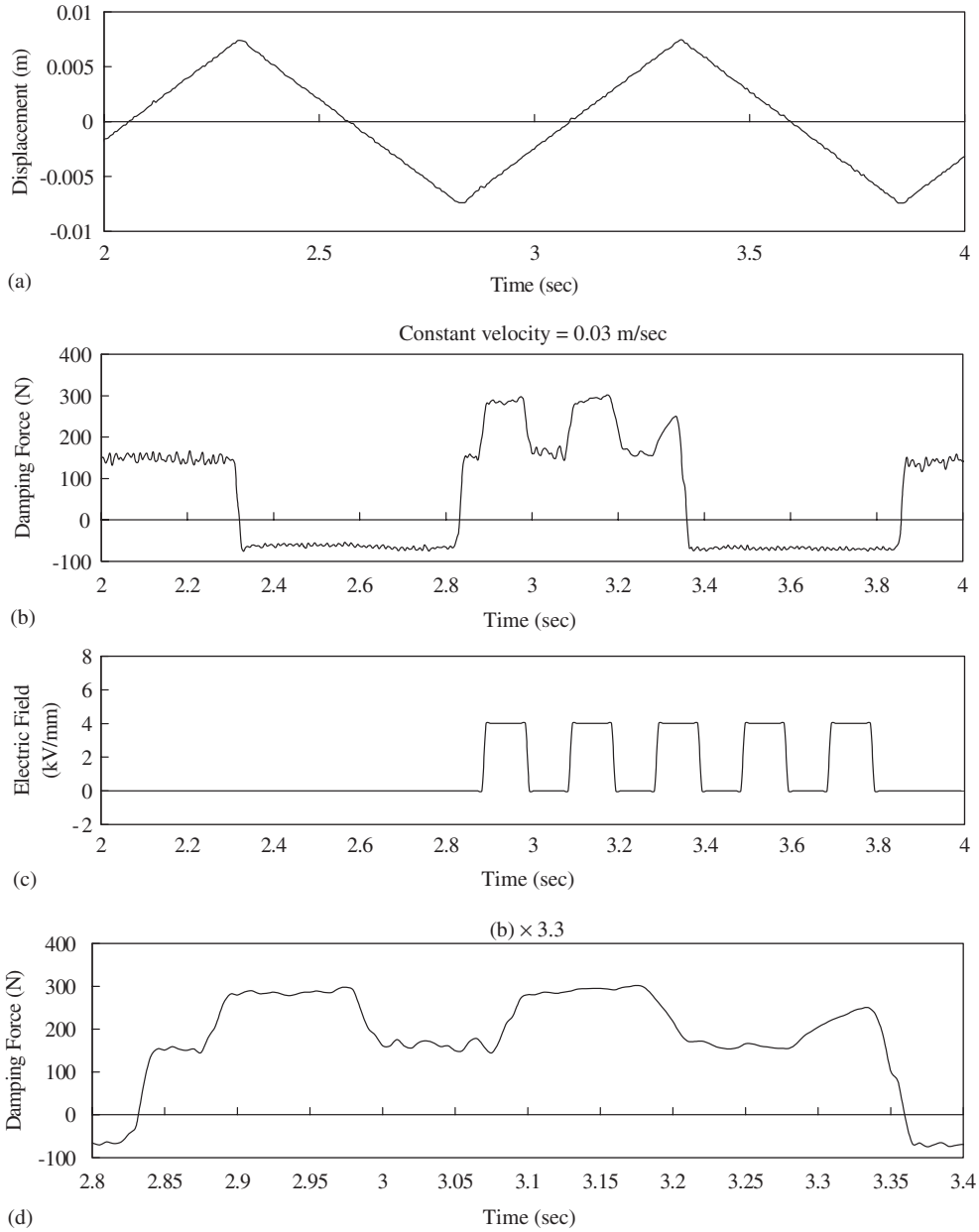

Fig. 11. Time response characteristics of the SMER damper to square wave control electric field. (a) The excitation triangular wave displacement of SMER damper ± 7.5 mm at 1 Hz frequency. (b) Transient response of SMER damper at velocity 28 mm/s. (c) The square wave control electric field 0–4 kV/mm at 5 Hz frequencies. (d) The partially magnified diagram of (b).

4. Performance evaluation of the SMER damper to control vibration system

In order to evaluate the performance of control vibration system using an SMER damper, we used a simple SDOF vibration system, as shown in Fig. 12, in which the sprung mass m_2 is isolated from the base. The mathematical model of the SDOF system from force equilibrium principle is

$$m_2\ddot{x}_2 = -k(x_2 - x_1) - C(E)(\dot{x}_2 - \dot{x}_1). \tag{21}$$

If the base excitation input function is $x_1(t) = x_0 \sin \omega t$, the transmissibility of displacement is defined as the ratio of the amplitude x_2 of the sprung mass m_2 to the input amplitude x_1 of the supporting base.

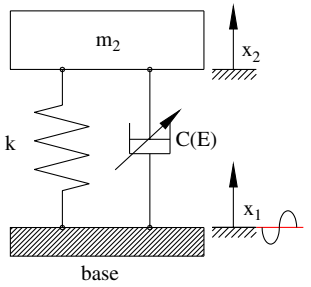

Fig. 12. An SDOF system.

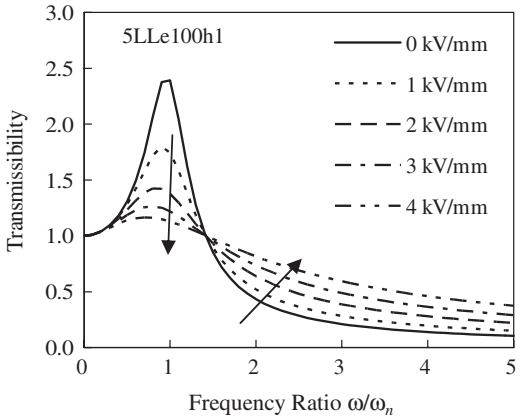

Fig. 13. Transmissibility of an SDOF system.

Transmissibility has both magnitude and phase, but we consider only the magnitude in this study. This is given by the relationship [31]:

$$|T| = \frac{|x_2|}{|x_1|} = \left\{ \frac{1 + (2\zeta r)^2}{(1 - r^2)^2 + (2\zeta r)^2} \right\}^{1/2}, \tag{22}$$

where ω is the exciting frequency, $\omega_n = \sqrt{k/m_2}$ is the natural frequency of the system and $\zeta = C/2m_2\omega_n$ is the damping ratio. $r = \omega/\omega_n$ is the frequency ratio. C, k and m_2 are the damping, stiffness and mass parameters indicated in Fig. 12. The damping coefficient $C(E)$ of the SMER damper is regulated by an electric field E, thus the damping ratio is a function of the electric field, i.e. $\zeta = f(E)$. The SMER damper has electrode numbers $n = 5$, electrode length $L_e = 100$ mm, electrode gap $h_e = 1$ mm and no check valve in the piston, and the parameters of SDOF system are $k = 70$ kN/m, $m_2 = 156$ kg. The controllable damping coefficient is applied to this vibration system. Fig. 13 shows the transmissibility against frequency ratio (ω/ω_n) for different values of damping ratio $\zeta = f(E)$ at a different electric field E, and this SMER damper is 5 L (electrode number 5) Le100 (electrode length 100 mm) h1(electrode gap 1 mm).

The schematic diagram of the testing device for control vibration system is shown in Fig. 14. The 3-layer SMER damper is installed on a hydraulic servo-dynamic tester. The top of the SMER damper is connected to a sprung mass, $m_2 = 156$ kg, which is mounted on two parallel guide rods, and the base is excited by a servo-valve cylinder. A 30 cm Novotechnik linear motion transducer is mounted to the exciting cylinder rod and the table frame to monitor the base displacement x_1, and another 30 cm Novotechnik linear motion transducer and TRANS-TEK linear velocity transducer are mounted to the table frame and sprung mass to monitor displacement x_2 and velocity $\dot{x}_2$ of sprung mass. A KYOWA accelerometer is mounted on the sprung mass to

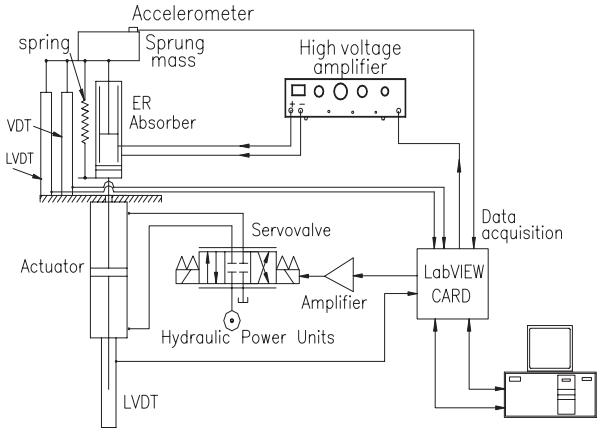

Fig. 14. The design of testing device for vibration control system.

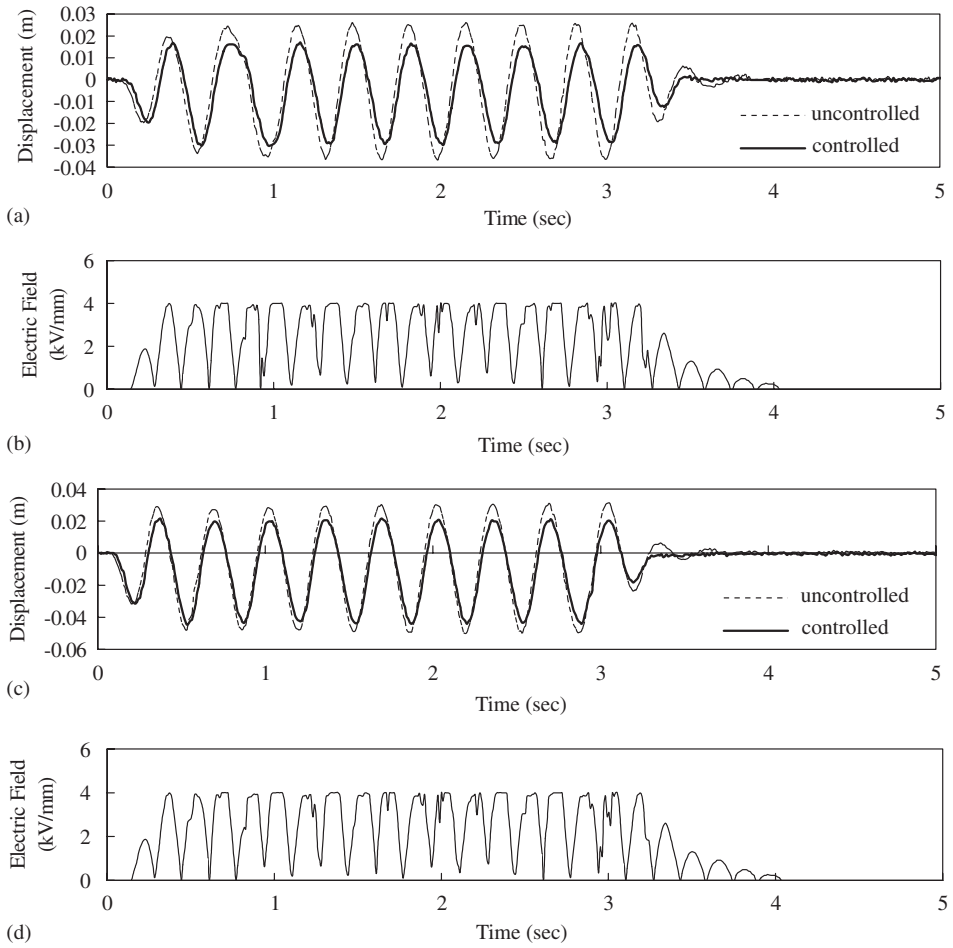

Fig. 15. The responses and input signals of a controlled vibration system. (a) The controlled and uncontrolled response for controlling the vibration system. The exciting input sine wave has a frequency of 3 Hz, and an amplitude of 12 mm, (b) the electric field input to the SMER damper of Fig. 15(a), (c) the controlled and uncontrolled response for controlling the vibration system. The exciting input sine wave has a frequency of 3 Hz, and an amplitude of 19 mm, and (d) the electric field input to the SMER damper of Fig. 15(c).

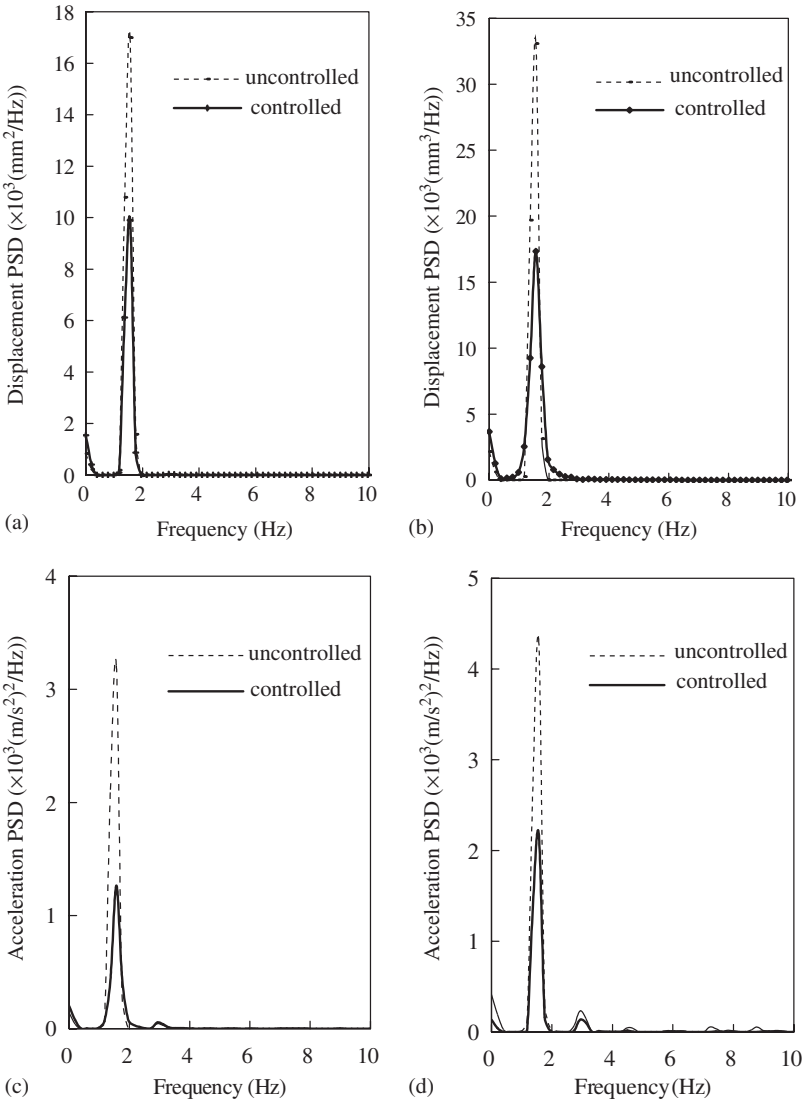

Fig. 16. Sine wave frequency responses of the vibration control system with the SMER damper. (a) Vertical displacement PSD with input sine wave amplitude 12 mm, (b) vertical displacement PSD with input sine wave amplitude 19 mm, (c) vertical acceleration PSD with input sine wave amplitude 12 mm, and (d) vertical acceleration PSD with input sine wave amplitude 19 mm.

monitor acceleration $\ddot{x}_2$ of the sprung mass. All data are collected using a National Instruments' data acquisition board and a personal computer.

The control system involves a controllable SMER damper and controller, but the vibration suppression is evaluated using an SMER damper without controller at first in this experimental study. The vibration system is suppressed by various electric field and exciting input amplitude and frequency. Then we have designed the proportional velocity controller, the control gain $E = k_v \dot{x}_2$. If $E \geqslant 4\,\mathrm{kV/mm}$, the maximum electric field is set by $E = 4\,\mathrm{kV/mm}$ to avoid the electrodes dielectric breakdown. This controller gain is $k_v = 15.12\,(\mathrm{kV/mm})/(\mathrm{m/s})$. Time delays of the ER fluid and the SMER damper can be ignored compared to the controlled frequency of the closed-loop vibration system.

Parameters of the vibration control system are sprung mass, $m_2 = 156\,\mathrm{kg}$; and spring constant, $k = 70\,\mathrm{kN/m}$. The test results are shown in Figs. 15 and 16 for controlling vibration system. Figs. 15(a) and (c) show the results for time responses using input sine wave. Figs. 15(b) and (d) show the electric field

input to the SMER damper. Fig. 16 shows the frequency responses obtained from power spectral density (PSD) of vertical displacement and acceleration of the sprung mass. It is clearly observed that the displacement and acceleration PSD are substantially reduced by more than 50% by applying the SMER damper and the controller.

5. Conclusions

This paper presents the design and performance evaluation of a serial multi-electrode electrorheological (SMER) damper. We describe the design method for ER dampers based on technical requirements of the damper such as controllable damping force, controllable ratio and the ratio of rebound damping force and compression damping force. An SMER damper is applied to a single-degree-of-freedom vibration system with a velocity control algorithm in order to evaluate the effectiveness of the controlling vibration system through computer simulation and experiments.

There are three main feature results in this study: (i) The controllable damping force and controllable ratio of the SMER damper are higher than that of single-electrode damper. (ii) A check valve on the piston is designed to meet the ratio of the damping force of the compression stroke to the damping force of the rebound stroke in the suspension system. (iii) The appropriate geometric size of electrodes can be designed for maximum controllable ratio and required damping force. This SMER damper can produce a relatively high damping force with short stroke and low effective ER fluid by selecting appropriate electrode length, electrode gap and number of electrodes.

In addition, semi-active vibration control systems equipped with the SMER dampers and motion controller are designed for the evaluation of the performance of the SMER dampers. The experimental results of the semi-active control system demonstrate that the displacement and the acceleration power spectral density are both significantly reduced by applying the semi-active control on the SMER dampers. The design and applications of SMER dampers as well as their optimal control algorithms for road vehicle suspension system will be our future research topics.

Acknowledgments

This research was sponsored by the National Science Council (NSC), Republic of China, Taiwan, under Contract No. NSC 90-2212-E-002-176. This financial support is greatly acknowledged.

References

[1] T.C. Halsey, J.E. Martin, Electrorheolgical fluids, *Scientific American* (1993) 42–49.
[2] K.D. Weiss, J.D. Carlson, J.P. Coulter, Material aspects of electro-rheological systems, *Journal of International Material Systems and Structures* 4 (1993) 13–34.
[3] N. Markis, S.A. Burton, D. Hill, M. Jordan, Analysis and design of ER damper for seismic protection of structures, *Journal of Engineering Mechanics* 10 (1996) 1003–1011.
[4] T.R. Weyenberg, J.W. Pialet, N.K. Petek, The development of ER fluids for an automotive semi-active suspension system, *International Journal of Modern Physics B* 10 (23 & 24) (1996) 3201–3209.
[5] T.M. Marksmeier, F. Gordaninejad, E.L. Wang, A. Stipanovic, Design and performance of an electrorheological grease shock absorber, *The Sixth International Conference on ERF/MRS and Their Applications*, 22–25 July, Yonezawa, Japan, 1997.
[6] T.M. Marksmeier, E.L. Wang, F. Gordaninejad, Theoretical and experimental studies of an electro-rheological grease shock absorber, *Journal of Intelligent Material Systems and Structures* 9 (1998) 693–703.
[7] N.D. Sims, R. Stanway, D.J. Peel, W.A. Bullough, A.R. Johnson, Controllable viscous damping: an experiment study of an electrorheological long-stroke damper under proportional feedback control, *Smart Materials and Structures* 8 (1999) 601–615.
[8] H.P. Gavin, Multi-duct ER dampers, *Journal of Intelligent Material Systems and Structures* 12 (2001) 353–366.
[9] G. Mui, D.L. Russell, J.Y. Wong, Nonlinear parameter identification of an ERF damper, *Journal of Intelligent Material Systems and Structures* 7 (1996) 560–564.
[10] N. Makris, S.A. Burton, D. Hill, M. Jordan, Analysis and design of ER damper for seismic protection of structures, *Journal of Engineering Mechanics* (1996) 1003–1011.
[11] W.H. Kuo, T.N. Wu, J. Guo, Y.N. Cheng, Study on the shock absorber using multielectrode electro-rheological valve, *Chinese Journal of Chemical Physics* 14 (5) (2001) 633–636 (in Chinese).
[12] H.P. Gavin, Design method for high-force electrorheological dampers, *Smart Material Structures* 7 (1998) 664–673.

[13] J.Y. Wong, X.M. Wu, M. Sturk, C. Bortolotto, On the application of ER fluid to the development of semi-active suspension systems for ground vehicles, *Transactions of the CSME* 17 (4B) (1993) 789–800.
[14] X.M. Wu, J.Y. Wong, M. Sturk, D.L. Russell, Simulation and experimental study of a semi-active suspension with an ER damper, *International Journal of Modern Physics B* 8 (1994) 2987–3003.
[15] M.J. Brennan, M.J. Day, R.J. Randall, An electrorheological fluid vibration damper, *Smart Materials and Structures* 4 (1995) 83–92.
[16] M. Nakano, A novel semi-active control of automotive suspension using an electrorheological shock absorber, in: *Proceedings of the Fifth International Conference on ER Fluid*, MR Suspensions and Associated Technology 1995, p. 645.
[17] R. Gordaninejad, A. Ray, H. Wang, Control of forced vibration using multi-electrode electro-rheological fluid dampers, *Journal of Vibration and Acoustics* 119 (1997) 527.
[18] S.B. Choi, Y.T. Choi, E.G. Chang, S.J. Han, C.S. Kim, Control characteristics of a continuously variable ER damper, *Mechatronics* 8 (1998) 143–161.
[19] M.S. Suh, M.S. Yeo, Development of semi-active suspension systems using ER fluids for the wheeled vehicle, *Journal of Intelligent Material Systems and Structures* 10 (1999) 743–747.
[20] J. Onoda, H.U. Oh, K. Minesugi, Improved electrorheological-fluid variable damper for semi-active vibration suppression, *AIAA Journal* 38 (2000) 1736.
[21] S.B. Choi, Y.T. Choi, D.W. Park, A sliding mode control of a full-car electrorheological suspension system via hardware in-the-loop simulation, *Transactions of the ASME* 122 (2000) 114–121.
[22] S.B. Choi, H.K. Lee, E.G. Chang, Field test results of a semi-active ER suspension system associated with skyhook controller, *Mechatronics* 11 (2001) 345–353.
[23] H.U. Oh, J. Onoda, An experimental study of a semiactive magneto-rheological-fluid variable damper for vibration suppression of truss structures, *Smart Materials and Structures* 11 (2002) 156.
[24] Y.N. Chen, T.N. Wu, W.H. Kuo, Y.C. Chung, Study on multi-electrode electrorheological fluid damper, in: *Proceedings of the 18th National Conference on Mechanical Engineering*, The Chinese Society of Mechanical Engineers, vol. 12, 2001, pp. 7–8, 419–426 (in Chinese).
[25] S.B. Choi, W.K. Kim, Vibration control of a semi-active suspension featuring electrorheological fluid dampers, *Journal of Sound and Vibration* 234 (3) (2000) 537–546.
[26] J. Dixson, *The Shock Absorber Handbook*, Society of Automotive Engineers Inc., USA, 1999 pp. 249–267.
[27] W.H. Kuo, T.N. Wu, J. Guo, Y.N. Chen, An experimental study on the multielectrode ER dampers, *Journal of Chinese Mechanical Engineering* 25 (1) (2004) 79–88.
[28] C. Wolff-Jesse, G. Fees, Examination of flow behavior of ERF in the flow mode, *Proceedings of the Institution of Mechanical Engineers* 212 (Part I) (1998) 159–173.
[29] H.E. Merritt, *Hydraulic control systems*, Wiley, New York, 1967 pp. 30–45.
[30] National Instruments, Ver.6.9.x, NI-DAQ for PC Compatibles, 2001.
[31] C.E. Crede, J.E. Ruzicka, Theory of vibration isolation, in: C.M. Harris (Ed.), *Shock and Vibration Handbook*, third ed., 1987 (Chapter 30).